

Comparative evaluation of hydrodynamic and gas–liquid mass transfer characteristics in bubble column and airlift slurry reactors

K.H. Choi, Y. Chisti *, M. Moo-Young

Department of Chemical Engineering, University of Waterloo, Waterloo, Ont. N2L 3G1, Canada

Received 30 October 1995; accepted 3 January 1996

Abstract

Three pneumatically agitated reactors – a bubble column and two airlift devices – with identical rectangular cross-sections ($0.456\text{ m} \times 0.153\text{ m}$), working heights (1.64 m) and equivalent gas sparging arrangements were compared in terms of the hydrodynamic and oxygen transfer performance. The two airlift reactors had identical riser-to-downcomer cross-sectional area ratios of 1.0, but differed in being sparged either in the central draft-tube or in the peripheral risers. The reactors produced comparable overall gas holdups for otherwise identical conditions in air–water or air–water–glass bead (0.069 mm particle diameter, 0%–5% (v/v) solids loading) systems. For the airlifts, irrespective of the sparging configuration or the solids loading, the same linear equation could relate the riser and the downcomer gas holdups. The velocity of the induced liquid circulation was not affected by solids loading, but the central draft-tube sparged design produced consistently higher velocities than did sparging in peripheral tubes. The bubble column had the poorest mixing performance. Complete suspension of solids occurred in all reactors in the range of superficial air velocities ($0.01\text{--}0.08\text{ m s}^{-1}$) tested; however, the distribution of solids was non-uniform in the bubble column. The airlift devices achieved homogeneous distribution. The oxygen transfer capability of the three reactors was comparable, with the bubble column performing slightly better.

Keywords: Bubble column; Airlift reactor; Hydrodynamics; Oxygen transfer; Mixing

1. Introduction

Bubble columns and airlift reactors are pneumatically agitated devices with numerous applications as gas–liquid–solid three-phase reactors. For example, in the chemical industry, gas–liquid reactions requiring heterogeneous catalysis, such as catalytic hydrogenations, are often carried out in slurry bubble columns [1,2]. In bioprocessing, airlift devices [3] are employed for microbial fermentation using suspended solid substrates, as well as in biological treatment of wastewater with microbial biofilms supported on suspended solid particles that enhance biomass concentration and retention [4]. Although slurry bubble columns are the most commonly used three-phase reactors and are the best studied [1,2], airlift reactors, with a well-defined flow pattern, are better suited to suspending solids. Information on three-phase airlift reactors is relatively sparse [3,5–16]. Particularly, few data exist on comparison of performance of bubble columns and airlift reactors in three-phase applications [3]. Further, among the airlift reactors, the draft-tube sparged mode of operation needs to be compared with the alternative of sparging in the

peripheral tubes. Because rectangular tank-type configurations are often simpler than cylindrical designs, rectangular configurations need to be examined in terms of the important operational parameters such as the suspension and distribution of solids, the overall gas holdup, the relationship between the riser and the downcomer gas holdup, the induced liquid circulation rates, mixing capability and oxygen transfer behaviour. Few studies are available on reactors with rectangular cross-sections [3,7,8,17–19] even though rectangular tank designs are the most common, especially in the wastewater treatment industry. In view of this lack of information, this work compares the performance characteristics of a bubble column and equivalent airlift devices with a rectangular geometry. Two modes of operation of airlift reactors are compared.

2. Experimental details

Three Plexiglas reactor configurations were used. All configurations had identical rectangular cross-sections and overall heights as shown in Fig. 1. Configuration (a) was a simple bubble column with the bottom corners filled in by two prisms

* Corresponding author.

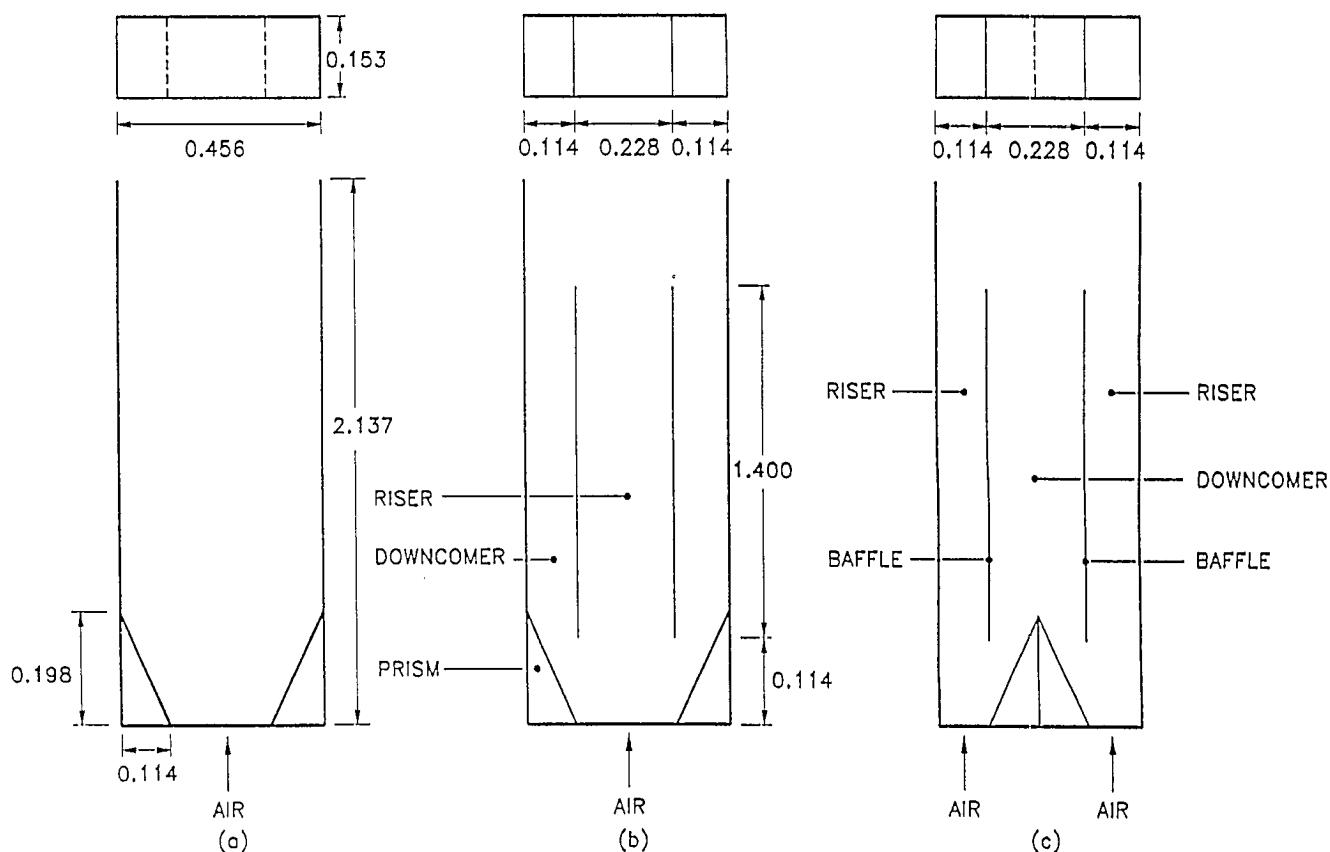


Fig. 1. Schematic diagrams of reactors: (a) bubble column; (b) draft-tube sparged airlift reactor; (c) airlift reactor with gas injection in outer tubes.

to eliminate dead zones. The internal angles between the sloping edges of the prisms and the base of the reactor were both 60° . Similar configurations had earlier been identified to reduce sedimentation of solids [20]. Configurations (b) and (c) were airlift devices. Configuration (b) was obtained by inserting two tightly fitting vertical baffles into the bubble column configuration (a). Configuration (c) was identical with configuration (b), except that the prisms were relocated to the centre as shown in Fig. 1 and air was now sparged in the peripheral risers instead of in the central riser of configuration (b). The three configurations were designed to enable a comparison of performance of otherwise geometrically equivalent bubble column and airlift reactors. Both the airlift reactors (b) and (c) had identical downcomer-to-riser cross-sectional area ratios of 1.0. In all cases the unaerated liquid–solid slurry height was identical at 1.64 m. The unaerated slurry volume was about 0.110 m^3 . Configurations (a) and (b) were sparged through identical perforated plates with 30 holes of 0.002 m diameter drilled on $0.0445 \text{ m} \times 0.0255 \text{ m}$ rectangular pitch. Equivalent spargers, each with 15 holes of 0.002 m diameter, were positioned at the bottoms of the two risers in configuration (c).

Tap-water and air were the liquid and gas phases respectively. The air flow rates were measured by a calibrated rotameter and the superficial gas velocity (U_G), based on the total cross-sectional area of the column, varied over $0.01\text{--}0.08 \text{ m s}^{-1}$ ($0.38\text{--}3.07 \text{ vvm}$). Glass beads with a mean particle diameter d_p of 0.069 mm, 95% sphericity and 2517 kg

m^{-3} density were the solid phase. The volume fraction of solids in the slurry ranged over 0–0.05. Batch operation was employed with respect to solid and liquid. All experiments were carried out at room temperature and atmospheric pressure.

For measurements, the reactors were filled with the liquid, a known amount of solids was added and the level of liquid was adjusted. Air was introduced at sufficient flow rate that all solid particles were suspended. The gas velocity was then gradually decreased to the desired levels and measurements were made after a minimum wait of 10 min to ensure that a hydrodynamic steady state had been attained [16].

The overall gas holdup ϵ was determined by visual measurements of the static slurry height h_L and the aerated height h_D . The gas holdup was calculated from the expression

$$\epsilon = \frac{h_D - h_L}{h_D} \quad (1)$$

The local gas holdups in the risers and downcomers of the airlift reactors were determined by measuring the hydrostatic pressure differences in these regions with inverted U-tube water manometers. The manometric taps were located in the risers and downcomers at 0.45 and 1.35 m from the baseplate in both cases. The solids concentration was measured by withdrawing samples of the slurry. Samples were taken midway between the manometric taps in the riser and downcomer. A syringe sample, r , with a large-bore needle (0.0015 m internal diameter) was used; the diameter of the bore was

more than 16-fold that of the particles. The needle was inserted up to the half-way point between the front and rear walls of the reactor. About 12 ml of slurry sample was collected over a short interval of about 2 s. The volume fraction of solids in the sampled slurry was determined from measurements of the sedimented or packed volume of the solids; thus

$$\phi_s = \frac{KV_P}{V_{SL}} \quad (2)$$

where V_{SL} is the total volume of the solid–liquid slurry sample and V_P is the packed volume of the solids. The constant K in Eq. (2) is the ratio of the actual volume V_S of solids and the packed volume [21]. For the solids used, the K value was experimentally determined to be 0.618. The gas holdups in the riser (ϵ_r) or the downcomer (ϵ_d) were calculated with the equation

$$\epsilon_r \text{ or } \epsilon_d = \frac{\rho_L \Delta h / \Delta z + \phi_s (\rho_s - \rho_L)}{\phi_s (\rho_s - \rho_L) + (\rho_L - \rho_G)} \quad (3)$$

which was derived by Wenge et al. [21]. In Eq. (3), ϕ_s is the measured volume fraction of solids in slurry samples, Δh is the manometer reading in the riser or the downcomer and Δz is the vertical distance between the measuring taps of manometers.

The liquid circulation velocity and mixing time were measured by the tracer impulse method [3]. Sodium hydroxide (2 kmol m^{-3}) and sulphuric acid (1 kmol m^{-3}) solutions (2 ml each) were alternately injected into the top of the reactor as tracers. The variations in pH were monitored with two pH probes and a chart recorder. The pH probes were installed in the downcomer in the airlift reactors. The mixing time was calculated from the response curves as the time required to achieve 90% of the final tracer concentration.

The overall volumetric oxygen transfer coefficient $k_L a_L$ was determined by the dynamic gassing-in method as used previously by Chisti and Moo-Young [18]. A polarographic dissolved oxygen electrode (Yellow Springs, YSI 5739) and a dissolved oxygen meter (YSI model 57) were used to follow the change in concentration of oxygen in a batch of slurry that had previously been freed of oxygen by bubbling through with nitrogen.

3. Results and discussion

As expected, because of the baffles, the macroscopic flow patterns in the airlift reactors differed significantly from those in the bubble column. In the airlift devices the usual [3] upflow in the riser(s) and downflow in the downcomer(s) occurred irrespective of the aeration rate. In the bubble column a well-defined bulk circulation of the liquid did not develop; several circulation cells were seen as shown in Fig. 2. A strong circulation cell developed near the base of the column (Fig. 2) at a low gas velocity of 0.02 m s^{-1} . The

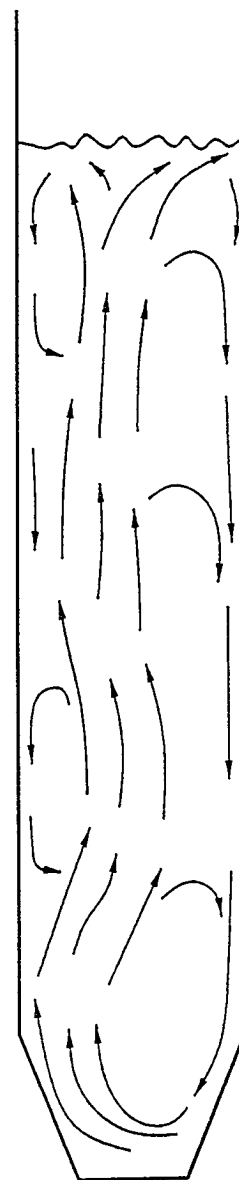


Fig. 2. Bulk liquid flow pattern in the bubble column.

slurry in the cell flowed upwards along one of the walls, while downflow occurred at the opposite wall (Fig. 2). Further increase in gas flow rate divided the large circulation cells into smaller ones or altered the size and location of the cells.

As shown in Fig. 3, for comparable conditions the overall gas holdups in the three reactor configurations were comparable, although there were small consistent differences. Because the hydraulic diameter of the riser in configuration (c) was smaller ($d_{r(c)} = 0.7d_{r(b)}$) than in configuration (b), the Reynolds numbers in the flow channels were correspondingly lower in configuration (c) for identical magnitudes of bulk fluid circulation in the two devices. Thus, for otherwise identical conditions, greater bubble coalescence occurred in the narrow and less turbulent risers of the airlift configuration (c). Consequently, the overall gas holdup in configuration (c) was about 5% lower than in configuration (b) (Fig. 3). These observations, while internally consistent, are in contrast with the findings of Koide et al. [12], who noted larger

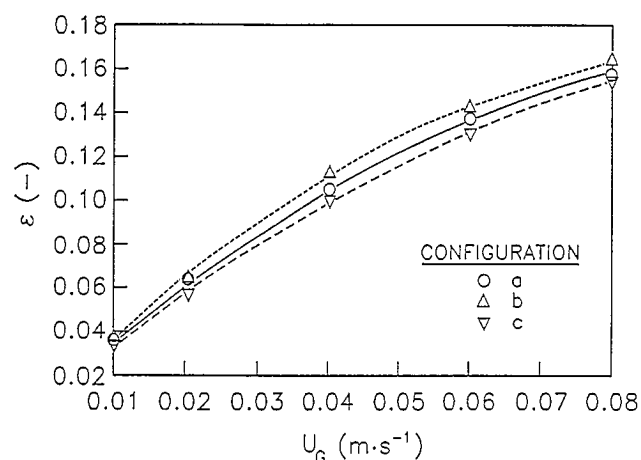


Fig. 3. Effect of superficial gas velocity on overall gas holdup for the three reactors (solids loading $\phi_s = 3\%$ (v/v)).

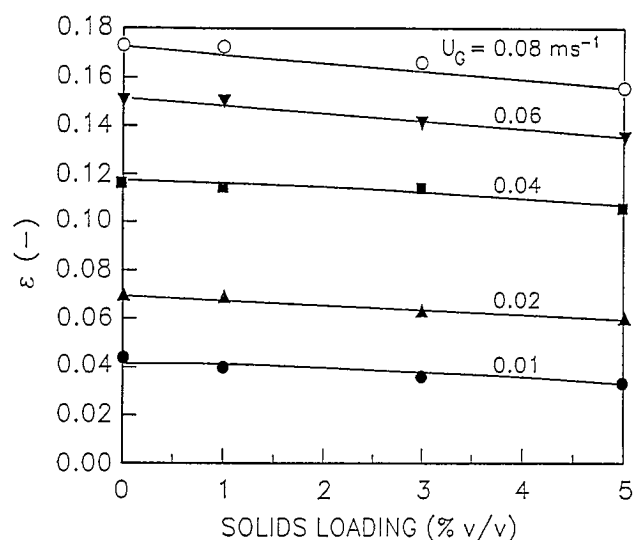


Fig. 4. Effects of solids loading and superficial gas velocity on overall gas holdup in airlift configuration (b).

Table 1
Parameters in Eq. (4) for the three reactors

Reactor type	α	β	γ
(a)	1.034	0.021	0.704
(b)	0.959	0.019	0.666
(c)	1.083	0.023	0.724

overall gas holdups in annulus sparged draft-tube airlift reactors than in equivalent devices that were sparged in the draft-tube.

The effect of solids loading on the overall gas holdup in configuration (b) is shown in Fig. 4 for various rates of gas flow. The solids loading ϕ_s in Fig. 4 is the volume percentage of solids placed in the solid-liquid two-phase slurry. Over the solids volume fraction range of 0%–5% (v/v), increasing solids loading caused marginal decline in the overall holdup. At any given solids loading the holdup increased with increasing gas flow rate, but the increase was smaller for the higher loadings (Fig. 4). Similar behaviour was noted for the gas holdup in the riser and the downcomer and in other reactor

configurations. The decline in holdup was associated with a larger mean bubble size and hence larger rise velocities of bubbles in slurries with increasing amounts of solids. The turbulence dampening effect of solids favoured bubble coalescence and a larger mean bubble diameter. This observation is consistent in principle with the results of Fan et al. [22] and Koide et al. [14] in other types of slurry reactors. The overall gas holdup data for all the reactor configurations tested were correlated with the equation

$$\epsilon = (\alpha - \beta\phi_s) U_G^\gamma \quad (4)$$

where ϕ_s is the input solids loading (volume percentage). The values of α , β and γ for the three reactors are given in Table 1. In all cases the non-linear correlation coefficients exceeded 0.995. Eq. (4) applied also to the two-phase system, i.e. when $\phi_s = 0$.

In airlift reactors the gas holdups in the riser and the downcomer have previously been shown to be linearly related. For example, Chisti [3] (p. 218) reported the empirical equation

$$\epsilon_d = 0.460\epsilon_r - 0.024 \quad (5)$$

for external-loop types of airlift reactors. Eq. (5) applied to aqueous salt solutions (0.15 kmol m^{-3} sodium chloride in water) with and without paper pulp fibre solids (1%–3% (w/v)) that were used to simulate mycelial fermentation broths. A similar equation was reported for suspensions of animal cell culture microcarrier support particles (0–10 kg m^{-3}) in split-cylinder internal-loop airlift reactors by Ganzeveld et al. [9]. The equation was

$$\epsilon_d = 0.63\epsilon_r - 0.0008 \quad (6)$$

Notice that Eqs. (5) and (6) are independent of the solids concentration. In the present work the data for the two airlift configurations fitted the equation

$$\epsilon_d = 0.988\epsilon_r - 0.016 \quad (7)$$

as shown in Fig. 5. Eq. (7) applied to solids-free as well as solids-containing operations over the entire range of solids loadings tested. Of particular note is the observation that for identical riser-to-downcomer cross-sectional area ratios, whether the airlift reactor is sparged in the draft-tube (configuration (b)) or in the outer tubes (configuration (c)) does not affect the relationship between the riser and downcomer gas holdups.

The variation in the superficial velocity (U_{Ld}) of liquid in the downcomer with increasing gas flow rates is depicted in Fig. 6 for the two airlift reactors. As shown in Fig. 6, by the time the gas flow had increased to 0.01 m s^{-1} , the induced liquid circulation rate had attained a constant value which was insensitive to further increase in gas flow until the flow exceeded 0.04 m s^{-1} . Beyond this value the flow regime transformed to churn turbulent flow and the consequent high gas holdup values in the riser caused a significant increase in the driving force for liquid circulation. Note that the airlift configuration (c) produced consistently lower values of liquid circulation velocities in comparison with configuration

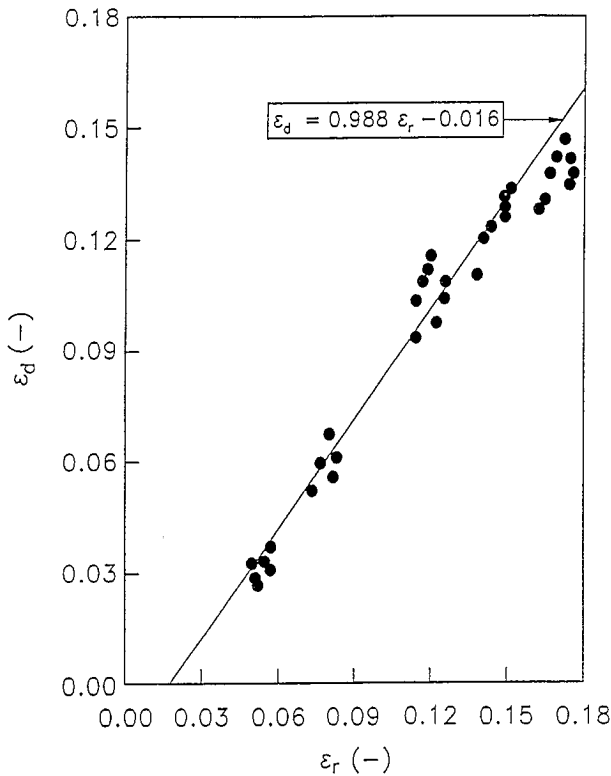


Fig. 5. Relationship between riser and downcomer gas holdups for the two airlift reactors.

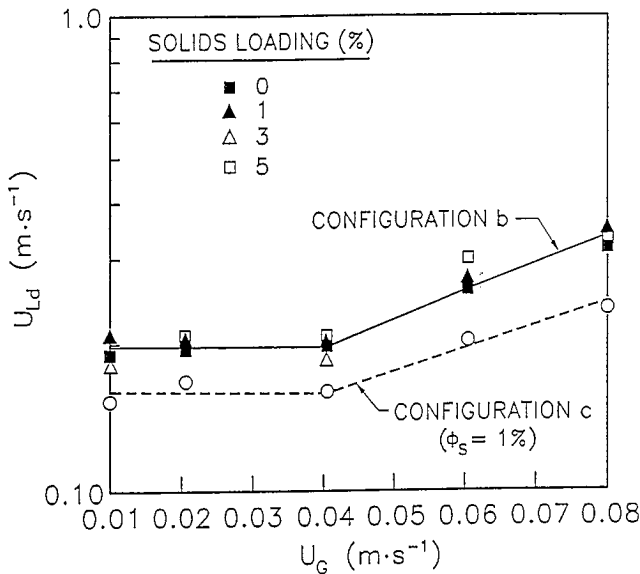


Fig. 6. Effects of superficial gas velocity and solids loading on induced liquid circulation velocity (U_{Ld}) in the two airlift devices.

(b). This behaviour was due to the higher pressure drop in the bottom zone of configuration (c) and the somewhat greater driving force for circulation in configuration (b). The latter was because of relatively higher Reynolds numbers and hence higher gas holdups in the riser of configuration (b).

Up to a solids loading of 5% (v/v) the solids did not have a significant impact on the magnitude of liquid circulation (Fig. 6). Previously, for substantially larger particles ($d_p = 0.4275$ mm) than used here but for a similar range of

solids loading ($\phi_s = 0.8\% - 4.0\%$), Livingston and Zhang [23] had reported a noticeable decrease in the liquid circulation rate with increasing loading of solids in a draft-tube airlift reactor.

Mixing in airlift reactors may be considered to have two contributing components: (i) backmixing due to recirculation and (ii) axial dispersion in the riser and the downcomer due to turbulence and differential velocities of the gas and liquid phases. The effect of superficial gas velocity on mixing time is shown in Fig. 7 for the three reactors. Over the solids loading range of 0%–5% (v/v) the loading had little effect on mixing time. The bubble column was the poorest mixed because of the lack of a well-defined bulk circulation of liquid. In the airlift reactors, mixing improved continuously with increasing gas flow rate (Fig. 7) even though the rate of induced liquid circulation was insensitive to gas flow velocity for velocities less than 0.04 m s⁻¹ (Fig. 6). Thus in the gas velocity range of $0.01 - 0.04$ m s⁻¹ the improvement in mixing was largely due to increasing axial dispersion; the contribution of circulatory flow loops was constant. In this range the relative velocity between the liquid and gas phases increased and, as pointed out by Weiland [24], the differences between the velocities of the phases are the main contributor to longitudinal mixing. The mixing times (Fig. 7) in airlift configuration (b) were about 10% lower than in configuration (c) and this was in keeping with the relative magnitudes of induced liquid circulation rates in the two devices (Fig. 6). The dependences of mixing time on gas velocity in airlift configurations (b) and (c) were correlated respectively with the equations

$$t_m = 13.714 U_G^{-0.277} \tag{8}$$

and

$$t_m = 11.243 U_G^{-0.360} \tag{9}$$

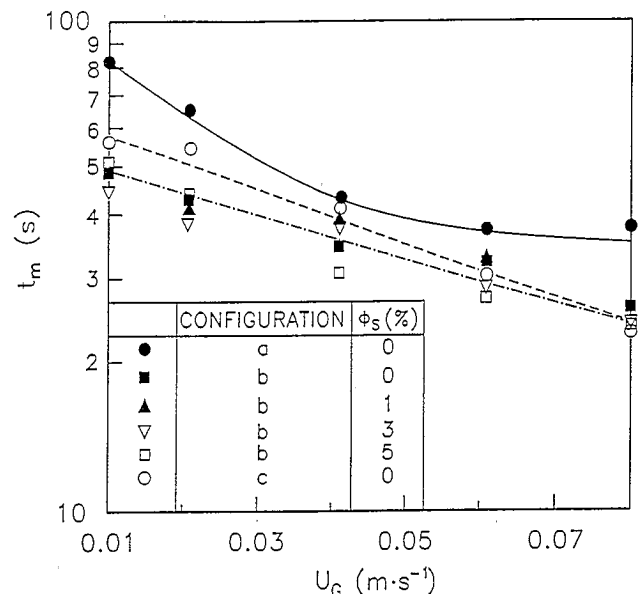


Fig. 7. Effects of superficial gas velocity and solids loading on mixing time (t_m) in the three reactor configurations.

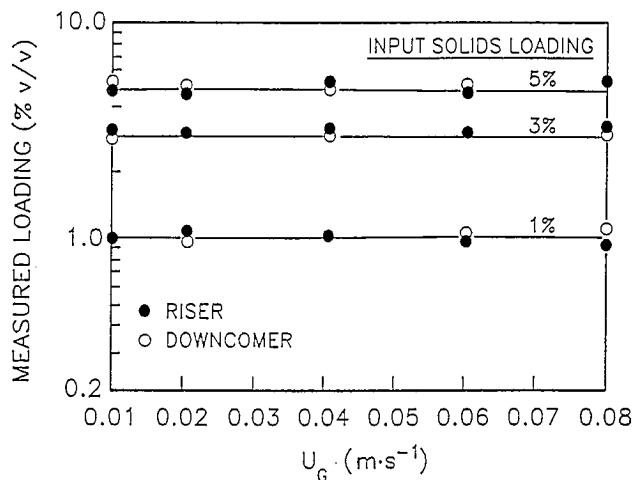


Fig. 8. Distribution of solids between riser and downcomer of airlift configuration (b) for various gas flow rates and input solids loadings.

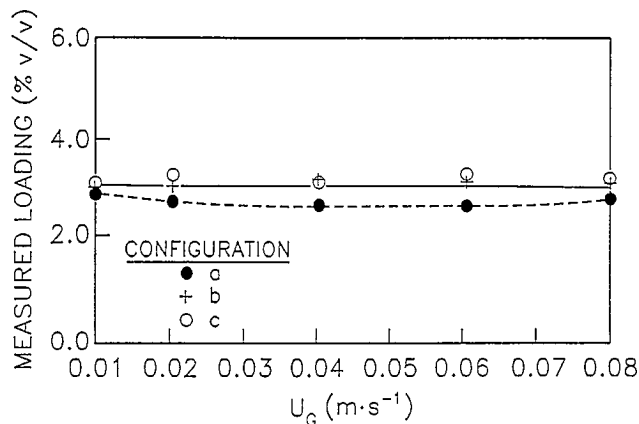


Fig. 9. Comparison of measured solids distribution in the three reactors for a total solids loading of 3% (v/v).

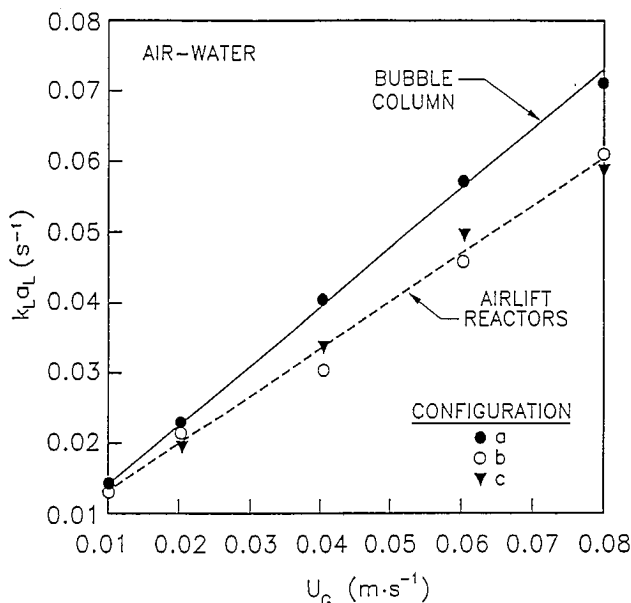


Fig. 10. Dependence of overall gas-liquid volumetric oxygen transfer coefficient on gas flow rate in the three reactor configurations.

The correlation coefficients for Eqs. (8) and (9) were 0.935 and 0.941 respectively.

Visual observations showed complete suspension of solids at superficial gas velocities of 0.01 m s^{-1} or higher in all reactors. As shown in Fig. 8 for airlift configuration (b), the measured distribution of solids was identical in the riser and the downcomer over the entire ranges of gas flow rates and input loadings of solids. Similar homogeneous dispersion of solids was observed in airlift configuration (c). These results were consistent with the uniform solids distribution noted by Wenge et al. [21] in a split-cylinder airlift reactor. Unlike in the airlift devices, the solids distribution in the bubble column was non-uniform. Thus, as shown in Fig. 9, for an input solids loading of 3% (v/v) the measured loadings were indeed 3% in the two airlift configurations but were lower in the bubble column at centre-line, 0.90 m above the sparger. Because complete suspension of solids was visually confirmed for the bubble column, the results in Fig. 9 implied a non-homogeneous distribution of solids. Other investigators have also reported axial variations in concentrations of suspended solids in slurry bubble columns [25].

The overall volumetric gas-liquid oxygen transfer coefficient $k_L a_L$ for the two airlift reactors was comparable as shown in Fig. 10; the bubble column gave somewhat higher values of $k_L a_L$ for otherwise identical conditions. In all cases $k_L a_L$ showed a linear dependence on gas flow rate in the range examined.

4. Conclusions

A bubble column and two airlift reactors with identical overall geometries were investigated as gas-liquid-solid three-phase reactors. The overall gas holdups produced in the reactors under identical conditions were similar; the draft-tube sparged mode of operation of the airlift gave somewhat higher holdups than did sparging in the peripheral channels. The overall holdup declined slightly with increasing loading of solids (0%–5% (v/v) solids loading). In the airlift reactors, irrespective of the solids loading or the mode of sparging, the riser and downcomer gas holdups were governed by the same linear relationship (Eq. (7)). The induced liquid circulation velocities in the draft-tube sparged reactor were higher than in the alternative mode of sparging because of the differences in pressure drops associated with the bottoms of the two airlift reactors. Despite this, the two reactors had comparable mixing performance whereas the bubble column proved to be a distinctly poorer mixer. All reactors achieved complete suspension of solids. The solids distribution in the two airlift devices was uniform, being identical in the risers and downcomers. The bubble column had a heterogeneous distribution of solids. In terms of oxygen transfer capability, the bubble column was marginally superior to the airlift reactors.

Acknowledgements

This work was funded by the Natural Sciences and Engineering Research Council of Canada. One of the authors (K.H.C.) was supported by the Korea Science and Engineering Foundation.

Appendix A: Nomenclature

d_p	particle diameter (m)
d_r	hydraulic diameter of riser ($4 \times$ flow area/wetted perimeter) (m)
Δh	manometer reading (m)
h_D	aerated slurry height (m)
h_L	unaerated slurry height (m)
$k_L a_L$	overall volumetric gas–liquid oxygen transfer coefficient (s^{-1})
K	constant ratio of actual volume to packed volume of solids
t_m	mixing time (s)
U_G	superficial gas velocity based on entire column cross-sectional area ($m\ s^{-1}$)
U_{LD}	superficial liquid velocity in downcomer ($m\ s^{-1}$)
V_P	packed volume of solid particles (m^3)
V_S	actual volume of solids (m^3)
V_{SL}	volume of solid–liquid slurry sample (m^3)
Δz	distance between manometer taps (m)

Greek letters

α	coefficient in Eq. (4)
β	coefficient in Eq. (4)
γ	exponent in Eq. (4)
ϵ	overall gas holdup
ϵ_d	downcomer gas holdup
ϵ_r	riser gas holdup
ρ_G	density of gas ($kg\ m^{-3}$)
ρ_L	density of liquid ($kg\ m^{-3}$)
ρ_S	density of solid particles ($kg\ m^{-3}$)
ϕ_S	volume fraction of solids in liquid–solid slurry

References

- [1] Y.T. Shah, B.G. Kelkar, S.P. Godbole and W.-D. Deckwer, Design parameters estimations for bubble column reactors, *AIChE J.*, **28** (1982) 353–379.
- [2] W.-D. Deckwer, *Bubble Column Reactors*, Wiley, New York, 1992.
- [3] Y. Chisti, *Airlift Bioreactors*, Elsevier Applied Science, London, 1989.
- [4] J.J. Heijnen, M.C.M. van Loosdrecht, A. Mulder and L. Tjihuis, Formation of biofilms in a biofilm airlift suspension reactor, *Water Sci. Technol.*, **26** (1992) 647–654.
- [5] J. Cai, Th.J. Nieuwstad and J.H. Kop, Fluidization and sedimentation of carrier material in a pilot-scale airlift internal-loop reactor, *Water Sci. Technol.*, **26** (1992) 2481–2484.
- [6] J. Cai and Th.J. Nieuwstad, Modelling the three-phase flow in a pilot-scale airlift internal-loop reactor for wastewater treatment, *Environ. Technol.*, **13** (1992) 101–113.
- [7] K.H. Choi, Y. Chisti and M. Moo-Young, Influence of the gas–liquid separator design on hydrodynamic and mass transfer performance of split-channel airlift reactors, *J. Chem. Technol. Biotechnol.*, **62** (1995) 327–332.
- [8] K.H. Choi, Y. Chisti and M. Moo-Young, Split-channel rectangular airlift reactors: enhancement of performance by geometric modifications, *Chem. Eng. Commun.*, **138** (1995) 171–181.
- [9] K.J. Ganzeveld, Y. Chisti and M. Moo-Young, Hydrodynamic behaviour of animal cell microcarrier suspensions in split-cylinder airlift bioreactors, *Bioprocess Eng.*, **12** (1995) 239–247.
- [10] M. Immich and U. Onken, Prediction of minimum gas velocity in suspended bubble columns and airlift reactors, *Chem. Eng. Sci.*, **47** (1992) 3379–3386.
- [11] K. Koide, H. Sato and S. Iwamoto, Gas holdup and volumetric liquid-phase mass transfer coefficient in bubble column with draft tube with gas dispersion into annulus, *J. Chem. Eng. Jpn.*, **16** (1983) 407–413.
- [12] K. Koide, K. Kurematsu, S. Iwamoto, Y. Iwata and K. Horibe, Gas holdup and volumetric liquid–phase mass transfer coefficient in bubble column with draft tube with gas dispersion into tube, *J. Chem. Eng. Jpn.*, **16** (1983) 413–419.
- [13] K. Koide, K. Horibe, H. Kawabata and S. Ito, Critical gas velocity required for complete suspension of solid particles in solid-suspended bubble column with draught tube, *J. Chem. Eng. Jpn.*, **17** (1984) 368–374.
- [14] K. Koide, K. Horibe, H. Kawabata and S. Ito, Gas holdup and volumetric liquid–phase mass transfer coefficient in solid-suspended bubble column with draft tube, *J. Chem. Eng. Jpn.*, **18** (1985) 248–254.
- [15] K. Muroyama, Y. Mitani and A. Yasunishi, Hydrodynamic characteristics and gas–liquid mass transfer in a draft tube slurry reactor, *Chem. Eng. Commun.*, **34** (1985) 87–98.
- [16] D. Petrović, D. Pošarac and A. Duduković, Minimum fluidization velocity of particles in draft tube airlift reactor, *Chem. Eng. Sci.*, **48** (1993) 2663–2667.
- [17] K. Akita and F. Yoshida, Gas holdup and volumetric mass transfer coefficient in bubble columns, *Ind. Eng. Chem. Process Des. Develop.*, **12** (1993) 76–80.
- [18] Y. Chisti and M. Moo-Young, Hydrodynamics and oxygen mass transfer in pneumatic bioreactor devices, *Biotechnol. Bioeng.*, **31** (1988) 487–494.
- [19] L.L. Gasner, Development and application of the thin channel rectangular airlift mass transfer reactor to fermentation and wastewater treatment systems, *Biotechnol. Bioeng.*, **16** (1974) 1179–1195.
- [20] M. Moo-Young, A.J. Daugulis, D.S. Chahal and D.G. Macdonald, The Waterloo process for SCP production from waste biomass, *Process Biochem.*, **14**(10) (1979) 38–40.
- [21] F. Wenge, Y. Chisti and M. Moo-Young, A new method for the measurement of solids holdup in gas–liquid–solid three-phase systems, *Ind. Eng. Chem. Res.*, **34** (1995) 928–935.
- [22] L.S. Fan, S.J. Hwang and A. Matsuura, Hydrodynamic behaviour of a draft tube gas–liquid–solid spouted bed, *Chem. Eng. Sci.*, **39** (1984) 1677–1688.
- [23] A.G. Livingston and S.F. Zhang, Hydrodynamic behaviour of three-phase (gas–liquid–solid) airlift reactors, *Chem. Eng. Sci.*, **48** (1993) 1641–1654.
- [24] P. Weiland, Influence of draft tube diameter on operation behaviour of airlift loop reactors, *Ger. Chem. Eng.*, **7** (1984) 374–385.
- [25] Y. Kato, A. Nishiwaki, T. Fukuda and S. Tanaka, The behaviour of suspended solid particles and liquid in bubble columns, *J. Chem. Eng. Jpn.*, **5** (1972) 112–118.